Title

Polymyxin B Resistance and Biofilm Formation in Vibrio cholerae Are Controlled by the Response Regulator CarR

Journal

Infection and Immunity, 83(3)

ISSN

0019-9567

Authors

Bilecen, Kivanc
Fong, Jiunn CN
Cheng, Andrew
et al.

Publication Date

2015-03-01

DOI

10.1128/iai.02700-14

Peer reviewed

IAI Journals.ASM.org

Polymyxin B Resistance and Biofilm Formation in *Vibrio cholerae* Are Controlled by the Response Regulator CarR

Kivanc Bilecen,* Jiunn C. N. Fong, Andrew Cheng, Christopher J. Jones, David Zamorano-Sánchez, Fitnat H. Yildiz

Department of Microbiology and Environmental Toxicology, University of California, Santa Cruz, Santa Cruz, California, USA

Two-component systems play important roles in the physiology of many bacterial pathogens. *Vibrio cholerae*'s CarRS two-component regulatory system negatively regulates expression of *vps* (*Vibrio* polysaccharide) genes and biofilm formation. In this study, we report that CarR confers polymyxin B resistance by positively regulating expression of the *almEFG* genes, whose products are required for glycine and diglycine modification of lipid A. We determined that CarR directly binds to the regulatory region of the *almEFG* operon. Similarly to a *carR* mutant, strains lacking *almE*, *almF*, and *almG* exhibited enhanced polymyxin B sensitivity. We also observed that strains lacking *almE* or the *almEFG* operon have enhanced biofilm formation. Our results reveal that CarR regulates biofilm formation and antimicrobial peptide resistance in *V. cholerae*.

Vibrio cholerae, a Gram-negative enteric pathogen, is the causative agent of the diarrheal disease cholera. To establish infection, *V. cholerae* senses and responds to host defenses encountered during the infection cycle. As an enteric pathogen, *V. cholerae* needs to launch a defense against antimicrobial peptides (APs), such as bactericidal permeability-increasing cationic protein (BPI), β-defensins, α-defensins, and cathelicidin (LL-37) produced in the human intestine (1, 2). It was shown that the outer membrane protein OmpU confers resistance to the P2 peptide derived from BPI and to pentacationic cyclic lipodecapeptides, synthesized by bacteria, known as polymyxin B (PMB). It does so by modulating the expression and activity of the alternative sigma factor sigma-E, which regulates the extracytoplasmic stress response (3, 4). Both BPI and polymyxin B are thought to interact with the lipid A moiety of lipopolysaccharide (LPS). In fact, lipid acylation catalyzed by MsbA/LpxN (VC0212), the genes for which encode a lipid A secondary hydroxyacyltransferase, and glycine and diglycine modification catalyzed by AlmG (VC1577), AlmF (VC1578), and AlmE (VC1579) were found to be critical for *V. cholerae* polymyxin B resistance (5, 6). It is proposed that a decrease in cell surface negative charge and membrane fluidity resulting from the glycine modification could impact antimicrobial peptide resistance. In addition to cell surface modifications, *V. cholerae* RND (resistance-nodulation-division) family efflux systems, in particular VexAB, contribute to polymyxin B resistance (7).

Two-component signal transduction systems (TCSs) play important roles in the physiology of many bacterial pathogens. A TCS is a phosphorelay-based signaling mechanism (8–10). The prototypical TCS consists of a membrane-bound histidine kinase (HK), which senses environmental signals, and a corresponding response regulator (RR), which mediates a cellular response. TCSs have been shown to contribute to increased resistance to antimicrobial peptides. The *Salmonella enterica* serovar Typhimurium PhoPQ TCS contributes to increased resistance to antimicrobial peptides. The response regulator PhoP regulates expression of genes, including *pagP*, *lpxO*, and *pagL*, which encode proteins involved in palmitoylation, hydroxylation, and deacetylation of lipid A, respectively (11–13). PhoPQ also activates *pmrAB* genes, which encode a TCS. PmrAB positively regulates expression of *pmrE* and *pmrHFIJKLM* genes, which are required for the addition of 4-amino-4-deoxy-L-arabinose (Ara4N) and phosphoethanolamine (PEtN) to the lipid A of LPS, and these modifications provide polymyxin B resistance (14, 15). In *Pseudomonas aeruginosa*, PhoPQ, PmrAB, and ParRS regulate polymyxin B resistance by upregulating the expression of the LPS modification operon *arnBCADTEF*. The proteins encoded by the *arn* genes catalyze the modification of LPS with Ara4N (16, 17). In *V. cholerae*, the regulatory mechanisms controlling resistance to antimicrobial peptides are not well understood.

We previously identified CarRS as negative regulators of biofilm formation in *V. cholerae* and here demonstrate that this TCS additionally plays a role in resistance to antimicrobial peptides (18). Biofilms—matrix-enclosed, surface-associated communities—are critical for environmental survival, transmission, and infectivity of *V. cholerae*. Extracellular matrix components, including polysaccharides (*Vibrio* polysaccharides [VPS]) (19) and matrix proteins (RbmA, RbmC, and Bap1) (20–22), connect cells and attach biofilms to environmental and host surfaces. *V. cholerae* biofilm formation is regulated by a complex network of interconnected regulatory elements (23, 24). VpsR is required for biofilm formation, as disruption of *vpsR* abolishes biofilm formation (25). The second positive regulator of biofilm formation is VpsT; its disruption reduces the biofilm-forming capacity of *V. cholerae* (26). CarR negatively regulates expression of *vpsR* and *vpsT* (18). *V. cholerae* biofilm formation is negatively regulated by

Received 27 September 2014 **Returned for modification** 2 November 2014
Accepted 6 January 2015

Accepted manuscript posted online 12 January 2015

Citation Bilecen K, Fong JCN, Cheng A, Jones CJ, Zamorano-Sánchez D, Yildiz FH. 2015. Polymyxin B resistance and biofilm formation in *Vibrio cholerae* are controlled by the response regulator CarR. Infect Immun 83:1199–1209. doi:10.1128/IAI.02700-14.

Editor: A. Camilli

Address correspondence to Fitnat H. Yildiz, fyildiz@ucsc.edu.

* Present address: Kivanc Bilecen, Okan University, Department of Genetic and Bio-engineering, Tuzla Campus, Akfirat-Tuzla, Istanbul, Turkey.

K.B., J.C.N.F., A.C., C.J.J., and D.Z.-S. contributed equally.

doi:10.1128/IAI.02700-14

TABLE 1 Bacterial strains and plasmids used in this study

Strain or plasmid	Relevant genotype	Reference or source
Strains		
E. coli		
CC118λ*pir*	Δ(*ara-leu*) *araD* Δ*lacX74 galE galK phoA20 thi-1 rpsE rpoB argE*(Am) *recA1* λ*pir*	42
S17-1λ*pir*	Tp^r Sm^r *recA thi pro* r_K^- m_K^+ RP4::2-Tc::MuKm Tn*7* λ*pir*	43
SM10λ*pir*	*thi thr leu tonA lacY supE recA* (RP4-2-Tc::Mu) λ*pir*R6K Km^r π^+	44
TOP10	F^- *mcrA* Δ(*mrr-hsdRMS-mcrBC*) ϕ80*lacZ*ΔM15 Δ*lacX74 recA1 araD139* Δ(*ara-leu*)*7697 galU galK rpsL* (Str^r) *endA1 nupG*	Invitrogen
BL21(DE3)	F^- *ompT* $hsdS_B(r_B^- m_B^-)$ *gal dcm* (DE3)	Invitrogen
V. cholerae		
FY_VC_1	*Vibrio cholerae* O1 El Tor A1552, wild type, Rif^r	45
FY_VC_3	Δ*lacZ* Rif^r	26
FY_VC_3282	Δ*carR* Rif^r	18
FY_VC_5668	Δ*almE* Rif^r	This study
FY_VC_4097	Δ*almF* Rif^r	This study
FY_VC_4094	Δ*almG* Rif^r	This study
FY_VC_5680	Δ*almEFG* Rif^r	This study
FY_VC_5486	Δ*carR* Δ*almEFG*, Rif^r	This study
FY_VC_237	Wild-type mTn*7-gfp* Rif^r Gm^r	46
FY_VC_3283	Δ*carR* mTn*7-gfp* Rif^r Gm^r	18
FY_VC_5563	Δ*almE* mTn*7-gfp* Rif^r Gm^r	This study
FY_VC_5762	Δ*almF* mTn*7-gfp* Rif^r Gm^r	This study
FY_VC_5758	Δ*almG* mTn*7-gfp* Rif^r Gm^r	This study
FY_VC_5687	Δ*almEFG* mTn*7-gfp* Rif^r Gm^r	This study
C6706	*Vibrio cholerae* O1 El Tor C6706, Str^r	47
FY_VC_3756	C6706 Δ*lacZ* Str^r	30
FY_VC_9419	C6706 Δ*carR* Str^r	This study
FY_VC_9744	C6706 Δ*almEFG* Str^r	This study
FY_VC_8466	C6706 mTn*7-gfp* Str^r Gm^r	This study
FY_VC_9750	C6706 Δ*almE* mTn*7-gfp* Str^r Gm^r	This study
FY_VC_9754	C6706 Δ*almEFG* mTn*7-gfp* Str^r Gm^r	This study
Plasmids		
pGP704*sacB*28	pGP704 derivative, *mob*/*oriT sacB* Ap^r	G. Schoolnik
pFY-119	pGP704-sac28::Δ*carR* Ap^r	18
pFY-985	pGP704-sac28::Δ*almE* Ap^r	This study
pFY-983	pGP704-sac28::Δ*almF* Ap^r	This study
pFY-981	pGP704-sac28::Δ*almG* Ap^r	This study
pFY-977	pGP704-sac28::Δ*almEFG* Ap^r	This study
pBAD/Myc-His B-C	Arabinose-inducible expression vector with C-terminal Myc epitope and six-His tags	Invitrogen
pFY-3601	p*carR* pBAD-Myc/His C::*carR* Ap^r	This study
pFY-705	p*almE* pBAD-Myc/His C::*almE* Ap^r	This study
pFY-703	p*almF* pBAD-Myc/His C::*almF* Ap^r	This study
pFY-701	p*almG* pBAD-Myc/His C::*almG* Ap^r	This study
pFY-1533	p*almEFG* pBAD-Myc/His B::*almEFG* Ap^r	This study
pBBR*lux*	*luxCDAB*-based promoter fusion vector, Cm^r	48
pFY-3448	pBBR-*almEFGp-lux*-1	This study
pFY-3449	pBBR-*almEFGp-lux*-2	This study
pFY-3450	pBBR-*almEFGp-lux*-3	This study
pFY-3451	pBBR-*almEFGp-lux*-4	This study
pUX-BF13	oriR6K helper plasmid, *mob*/*oriT*, provides the Tn*7* transposition function in *trans*, Ap^r	49
pMCM11	pGP704::mTn*7-gfp* Gm^r Ap^r	M. Miller and G. Schoolnik

HapR, a master quorum sensing regulator, and cyclic AMP (cAMP) and cAMP binding protein (CRP) (27–30). Our previous work showed that the CarRS system acts in parallel with HapR to repress biofilm formation. Whole-genome expression profiling of *carR* and *carS* mutants revealed that CarRS regulates the transcription of the *almEFG* operon (18), whose products are involved in the synthesis of glycine-modified lipid A species in *V. cholerae* (5, 18) and in polymyxin B resistance.

In this study, we report that CarR positively regulates *almEFG* by directly binding to the regulatory region of the *almEFG* operon. Expression of *almEFG*, in turn, promotes polymyxin B resistance. We also provide evidence that similarly to CarR, AlmE contributes

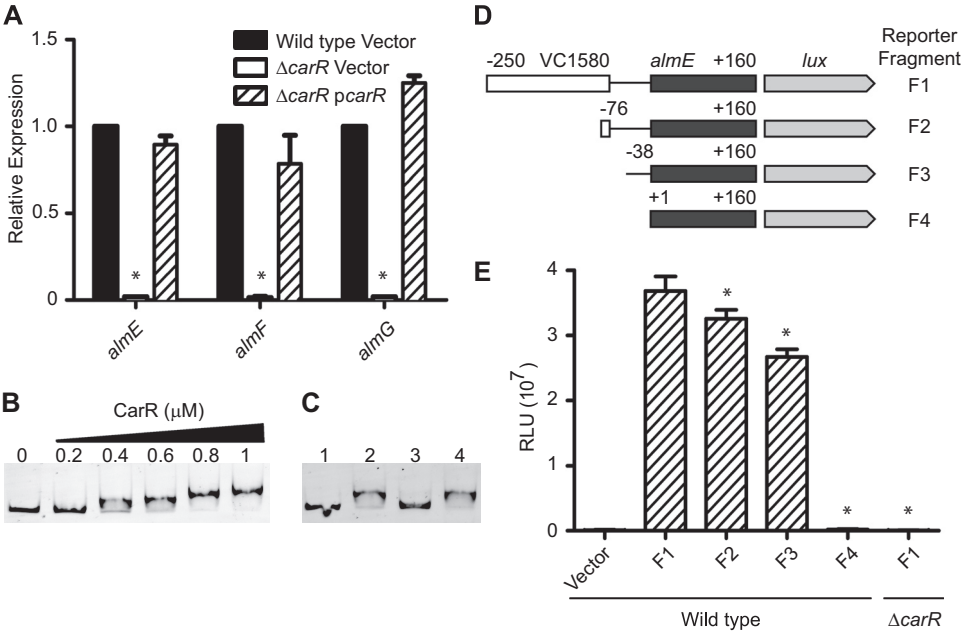

FIG 1 Regulation of *almEFG* expression. (A) Relative expression of *almE*, *almF*, and *almG* mRNA levels measured via qRT-PCR in A1552 wild type and the Δ*carR* strain harboring vector only (pBAD/Myc-His C) or the complementation plasmid p*carR*. Data are normalized to the *recA* expression via the Pfaffl method, with the expression of the wild type set to 1.0. The graph represents the mean expression of two independent experiments performed in triplicate. Statistical significance was determined with Student's *t* test; asterisks indicate *P* values of <0.01. Error bars represent standard deviations. (B) CarR binds to the *almEFG* promoter region. Mobility shift assays performed with the *almEFG* promoter region and $_{VIC}alm_{FAM}$, with different concentrations (0, 0.2, 0.4, 0.6, 0.8, and 1 μM) of the response regulator CarR. (C) DNA binding by CarR is specific to the *almEFG* regulatory region. Lane 1, free fluorescent probe $_{VIC}alm_{FAM}$ (0.005 μM); lane 2, fluorescent probe $_{VIC}alm_{FAM}$ (0.005 μM) plus 0.8 μM CarR; lane 3, fluorescent probe $_{VIC}alm_{FAM}$ (0.005 μM) plus 0.8 μM CarR and 56× unlabeled probe *alm*; lane 4, fluorescent probe $_{VIC}alm_{FAM}$ (0.005 μM) plus 0.8 μM CarR and 56× $cyaA_{Cy3}$ unspecific probe. (D) Schematic representation of the reporter fragments (F1 to F4) used to analyze the expression of the *almEFG* operon. The coordinates correspond to the position with respect to the annotated start codon. Rectangles and arrows represent the structural genes. (E) Expression of various *almEFGp-lux* reporter fragments (F1 to F4) in A1552 wild-type and Δ*carR* strains shown in relative luminescence units (RLU; counts min^{-1} ml^{-1}/OD_{600}). The graph represents the mean expression of two independent experiments performed with four replicates. Statistical significance was determined using a one-way ANOVA and Dunnett's multiple-comparison test; asterisks indicate *P* values of <0.01. Error bars represent standard deviations.

to repression of biofilm formation in *V. cholerae* and that CarR contributes to intestinal colonization in a strain-specific manner.

MATERIALS AND METHODS

Bacterial strains, plasmids, and culture conditions. The bacterial strains and plasmids used in this study are listed in Table 1. All *V. cholerae* and *Escherichia coli* strains were grown aerobically, at 30°C and 37°C, respectively, unless otherwise noted. All cultures were grown in Luria-Bertani (LB) broth (1% tryptone, 0.5% yeast extract, 1% NaCl), pH 7.5, unless otherwise noted. LB agar medium contains 1.5% (wt/vol) granulated agar (BD Biosciences, Franklin Lakes, NJ). Concentrations of antibiotics and inducers used, when appropriate, were as follows: ampicillin, 100 μg/ml; rifampin, 100 μg/ml; streptomycin, 100 μg/ml; gentamicin, 50 μg/ml; chloramphenicol, 20 μg/ml (*E. coli*) or 5 μg/ml (*V. cholerae*); and arabinose, 0.2% (wt/vol). In-frame deletion and green fluorescent protein (GFP)-tagged strains were generated according to protocols previously published (20, 21).

Recombinant DNA techniques. DNA manipulations were carried out by standard molecular techniques according to the manufacturer's instructions. Restriction and DNA modification enzymes were purchased from New England BioLabs (NEB, Ipswich, MA). PCRs were carried out using primers purchased from Bioneer Corporation (Alameda, CA) and the Phusion high-fidelity PCR kit (NEB, Ipswich, MA), unless otherwise noted. Sequences of the primers used in the present study are available upon request. Sequences of constructs were verified by DNA sequencing (UC Berkeley DNA Sequencing Facility, Berkeley, CA).

RNA isolation. Total RNA was isolated from *V. cholerae* cells according to a previously published protocol (24). Briefly, overnight-grown cultures of *V. cholerae* in LB medium supplemented with ampicillin at 30°C were diluted 1:200 in LB medium supplemented with ampicillin and 0.2% arabinose and incubated at 30°C with shaking at 200 rpm until they reached an optical density at 600 nm (OD_{600}) of 0.3 to 0.4. To ensure homogeneity, these cultures were diluted again 1:200 in LB medium supplemented with ampicillin and 0.2% arabinose and grown to an OD_{600} of 0.3 to 0.4. Aliquots (1.8 ml) were collected by centrifugation, immediately resuspended in 1 ml of TRIzol reagent (Life Technologies, Carlsbad, CA), and stored at −80°C. These samples were incubated for 5 min at room temperature, and 0.2 ml of chloroform was added into each tube. Tubes were shaken, incubated at room temperature for 5 min, and then centrifuged for 20 min at 12,000 × *g* and 4°C. The aqueous layer was removed into a new tube. Isopropanol (250 μl) and 250 μl high-salt solution (0.8 M sodium citrate, 1.2 M NaCl) were added, and the suspension was incubated for 10 min at room temperature to precipitate the RNA. Isopropanol was removed after centrifugation for 30 min at 12,000 × *g* and 4°C. Pellets were washed with 1 ml of 75% ethanol, and ethanol was removed after centrifugation for 5 min at 7,500 × *g* and 4°C. Pellets were dried at room temperature for 10 min. Dried pellets were then resuspended in RNase-free water. To remove contaminating DNA, total RNA was incubated with Turbo DNase (Life Technologies, Carlsbad, CA), and the RNeasy minikit (Qiagen, Valencia, CA) was used to clean up the RNA after DNase digestion.

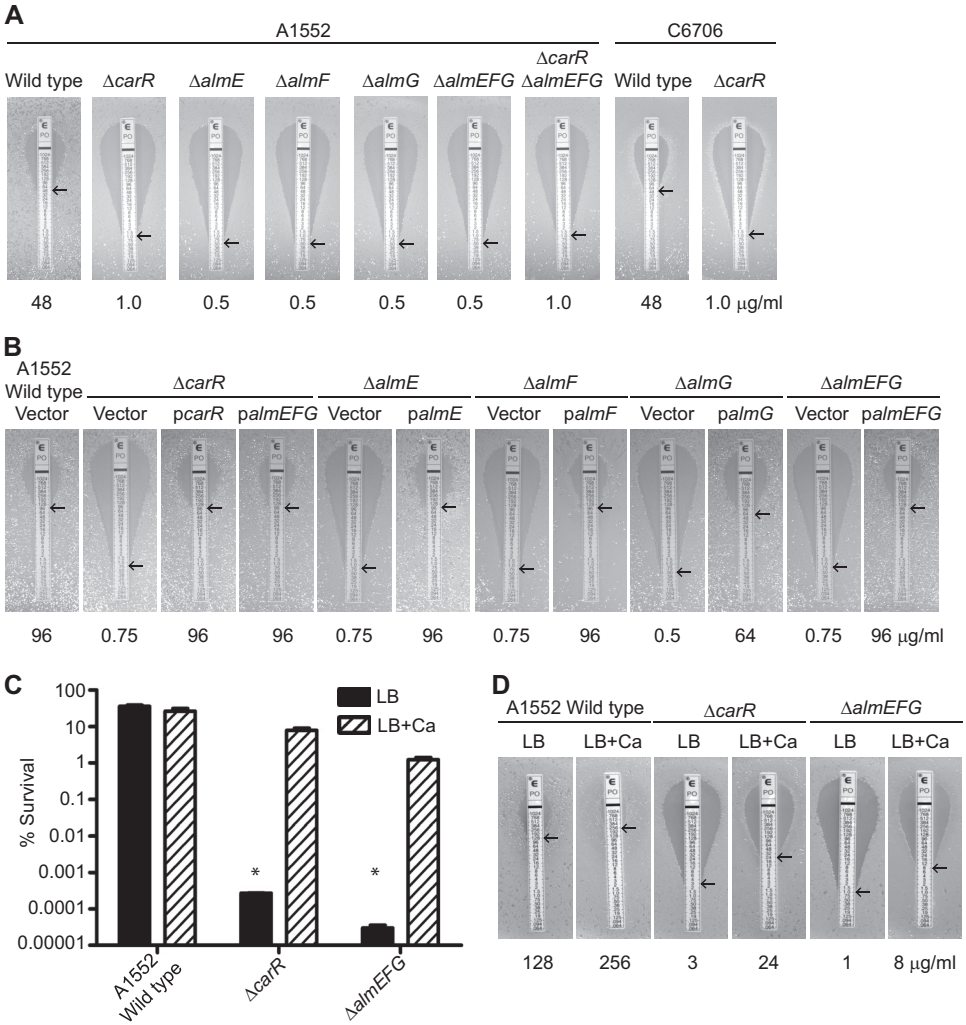

FIG 2 Polymyxin B sensitivity of wild-type, *carR*, and *almEFG* strains. (A) Polymyxin B MIC assays of wild-type and mutant (Δ*carR*, Δ*almE*, Δ*almF*, Δ*almG*, Δ*almEFG*, and Δ*carR* Δ*almEFG*) strains in A1552 and C6706 genetic backgrounds. (B) Polymyxin B MIC assay of A1552 wild-type and mutant strains harboring vector only or complementation plasmids. (C) Polymyxin B killing assays of A1552 wild-type and Δ*carR* and Δ*almEFG* strains grown in the presence or absence of Ca^{2+}. % survival = $(CFU_{PMB\ treatment}/CFU_{no\ treatment}) \times 100$. Statistical significance was determined with Student's *t* test; asterisks indicate *P* values of <0.05. Error bars represent standard deviations. (D) Polymyxin B MIC assays of A1552 wild-type, Δ*carR*, and Δ*almEFG* strains grown in the presence or absence of Ca^{2+}. Arrows indicate the MIC (μg/ml) on Etest gradient polymyxin B strips; MIC values are shown below the images. Assays were carried out with at least 2 biological replicates and 2 technical replicates.

Quantitative reverse transcription real-time PCR (qRT-PCR). The SuperScript III first-strand synthesis system (Life Technologies, Carlsbad, CA) was used to synthesize cDNA from 1 μg of isolated total RNA. Real-time PCR was performed using a Bio-Rad CFX1000 thermal cycler and Bio-Rad CFX96 real-time imager with specific primer pairs (designed within the coding region of the target genes) and SsoAdvanced SYBR green supermix (Bio-Rad, Hercules, CA). Results are from two independent experiments performed in triplicate. All samples were normalized to the expression of the housekeeping gene *recA* via the Pfaffl method (31). Statistical analysis was performed using a one-way analysis of variance (ANOVA) with Bonferroni's multiple-comparison test.

Protein production and purification. The coding region of *carR*, excluding the stop codon, was amplified by PCR and cloned into the pBAD/Myc-His C bacterial expression vector (Life Technologies, Carlsbad, CA), resulting in an overexpression plasmid encoding a recombinant CarR protein with a C-terminal Myc and 6×His tags (CarR-mycHis). The *carR* overexpression plasmid (p*carR*) was transformed into *E. coli* strains TOP10 and BL21(DE3) for maintenance and protein production, respectively. CarR-mycHis was purified by metal affinity purification using a Talon resin (Clontech Laboratories, Mountain View, CA) according to the manufacturer's instructions. Briefly, cultures of BL21(DE3) harboring p*carR* were grown to mid-exponential phase in LB medium supplemented with ampicillin at 37°C, and expression of the recombinant protein was induced for 3 h at 30°C with the addition of 0.2% arabinose. Cells were harvested and then lysed with xTractor buffer (20 ml/g) (Clontech Laboratories, Mountain View, CA) for 10 min with orbital agitation at 4°C. The crude extract was centrifuged at 4°C to obtain the clarified sample (soluble fraction). The protein was purified with a batch/gravity flow protocol at 4°C using preequilibrated Talon resin (equilibration buffer: 50 mM sodium phosphate, 300 mM NaCl; pH 7.4). Elution of the protein was achieved by adding 250 mM imidazole to the equilibration buffer. To remove imidazole, the purification buffer was exchanged for a storage buffer (137 mM NaCl, 2.7 mM KCl, 10 mM Na_2HPO_4, 2 mM KH_2PO_4, pH 7.0, 20% glycerol) using an Amicon Ultra-0.5-ml 10K centrifugal filter (Millipore, Billerica, MA). Protein concen-

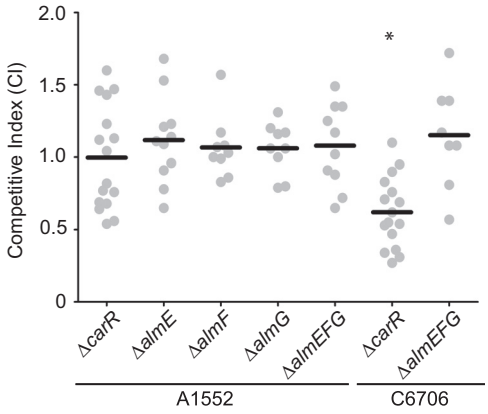

FIG 3 Intestinal colonization of wild-type, *carR*, and *almEFG* strains. Wild type (A1552 or C6706) was coinoculated with Δ*carR*, Δ*almE*, Δ*almF*, Δ*almG*, and Δ*almEFG* mutants at a ratio of ~1:1 into infant mice. The number of bacteria per intestine was determined 20 to 22 h postinoculation. The competitive index (CI) was determined as the output ratio of mutant to wild type divided by the input ratio of mutant to wild type. Each dot represents data from an individual mouse. Statistical analysis was performed using Student's two-tailed *t* test; the asterisk indicates a *P* value of <0.05.

tration was determined using the Coomassie Plus (Bradford) protein assay (Thermo Scientific, Rockford, IL) and bovine serum albumin (BSA) as standards.

Electrophoretic mobility shift assays (EMSAs). A DNA fragment encompassing the regulatory region (−250 to +160 bp with respect to the translational start site) of the *almEFG* operon was amplified using a forward oligonucleotide (GTTGCGTCTATTGGCGCG) labeled at the 5′ end with the fluorescent dye VIC, which has an absorbance maximum of 538 nm and an emission maximum of 554 nm (Life Technologies Corporation, Grand Island, NY), and a reverse oligonucleotide (TCTGTTTAA CCCATAATGCAGGG) labeled at the 5′ end with the fluorescent dye 6-carboxyfluorescein (FAM), which has an absorbance maximum of 492 nm and an emission maximum of 517 nm (Life Technologies Corporation, Grand Island, NY). The amplified product was purified using the Wizard SV gel and PCR cleanup system (Promega, Madison, WI), and the concentration was determined using a NanoDrop spectrophotometer (Thermo Scientific, Rockford, IL). Prior to binding, the recombinant CarR protein (2 μM) was incubated in a buffer containing 100 mM Tris-Cl (pH 7.0), 10 mM $MgCl_2$, 125 mM KCl, and 50 mM disodium carbamoyl phosphate (Sigma, St. Louis, MO) for 1 h at 30°C. For the binding reactions, the fluorescently labeled probe (0.005 μM) and CarR (from 0.2 to 1 μM) were combined in a binding buffer [100 mM Tris-Cl (pH 7.4), 100 mM KCl, 10 mM $MgCl_2$, 10% glycerol, 2 mM dithiothreitol, 20 ng/μl poly(dI-dC), and 50 ng/μl of bovine serum albumin [BSA]) and incubated for 30 min at room temperature. The binding reaction mixtures were immediately loaded into a 5% acrylamide gel (37:5:1) and run at 4°C in 0.5× Tris-borate-EDTA buffer (Bio-Rad, Hercules, CA) for 30 min at 150 V. The competition assays were performed by incubating CarR (0.8 μM) and the labeled probe (0.005 μM) in the presence of unlabeled specific probe (0.28 μM) or a Cy3-labeled *cyaA* (−253 to −43 bp) nonspecific probe (0.28 μM). DNA migration was visualized using a ChemiDoc MP imaging system (Bio-Rad, Hercules, CA) with a 530/28 filter with Blue Epi illumination to limit detection of the Cy3 fluorophore (filter 605/50 Green Epi illumination).

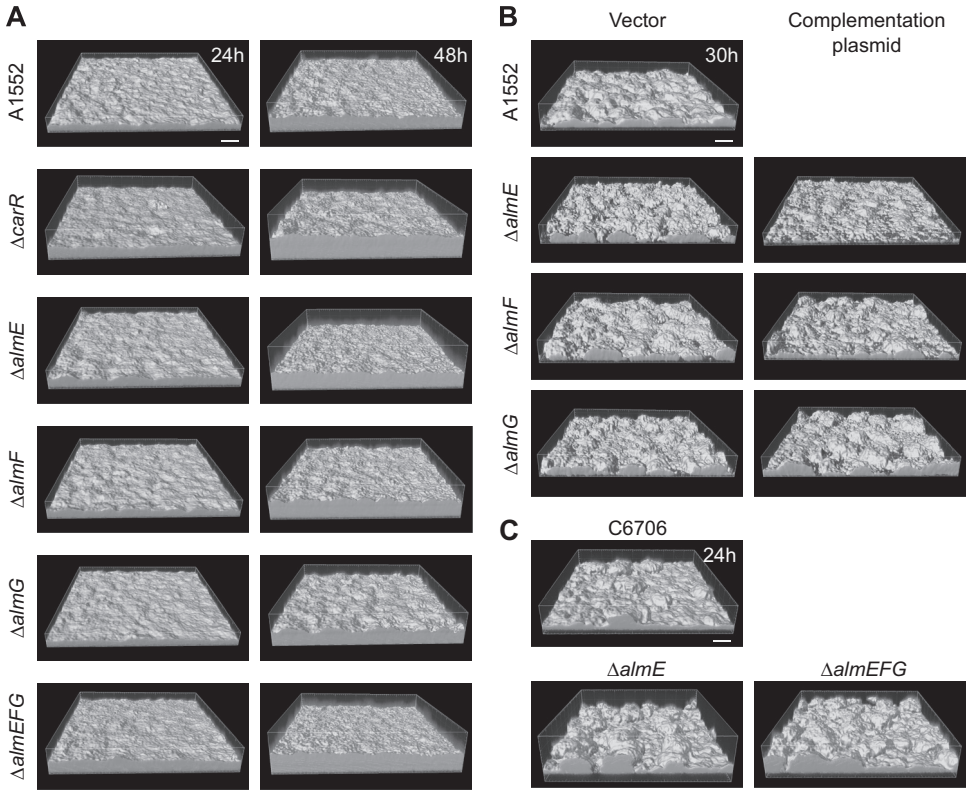

FIG 4 Biofilm formation of *alm* mutants and complemented strains. (A) Three-dimensional view of biofilms formed by A1552 wild type and Δ*carR*, Δ*almE*, Δ*almF*, Δ*almG*, and Δ*almEFG* mutants after 24 h and 48 h. (B) Biofilms formed by A1552 wild type harboring the empty vector and *alm* deletion strains harboring empty vector or respective complementation plasmids. Biofilms were grown in flow cells for 30 h and stained with Syto-9 prior to confocal imaging. (C) Biofilms formed by wild-type C6706 and Δ*almE* and Δ*almEFG* strains in the C6706 genetic background after 24 h. Bars, 40 μm.

TABLE 2 COMSTAT quantitative analysis of biofilms formed after 24 h and 48 h by wild-type A1552 and *almEFG* mutants

Strain	Mean (SD) and significance at[a]: 24 h									
	Biomass	Significance	Avg thickness (μm)	Significance	Maximum thickness (μm)	Significance	Substrate coverage[b]	Significance	Roughness	Significance
Wild type	9.75 (0.98)		9.01 (0.90)		15.11 (2.85)		1.00 (1.0×10^{-3})		0.14 (0.02)	
Δ*carR* mutant	13.19 (1.34)	***	12.56 (1.25)	***	20.46 (6.05)	**	1.00 (2.00×10^{-6})	NS	0.11 (0.02)	NS
Δ*almE* mutant	10.89 (1.68)	NS	10.21 (1.57)	NS	16.50 (2.60)	NS	1.00 (5.20×10^{-6})	NS	0.14 (0.04)	NS
Δ*almF* mutant	10.31 (1.31)	NS	9.60 (1.17)	NS	15.18 (3.03)	NS	1.00 (5.63×10^{-6})	NS	0.13 (0.03)	NS
Δ*almG* mutant	9.50 (0.75)	NS	8.78 (0.72)	NS	14.30 (1.64)	NS	1.00 (6.93×10^{-5})	NS	0.14 (0.03)	NS
Δ*almEFG* mutant	12.61 (2.04)	***	11.97 (1.94)	***	18.85 (4.08)	NS	1.00 (6.14×10^{-6})	NS	0.11 (0.02)	NS

Confocal laser scanning microscopy (CLSM) and flow cell biofilm studies. Inoculation of flow cells was done by normalizing overnight-grown cultures to an OD_{600} of 0.02 and injecting cells into an Ibidi m-Slide VI0.4 (Ibidi 80601; Ibidi LLC, Verona, WI). To seed the flow cell surface, bacteria were allowed to adhere at room temperature for 1 h. Flow of 2% (vol/vol) LB (0.2 g/liter tryptone, 0.1 g/liter yeast extract, 1% NaCl) was initiated at a rate of 7.5 ml/h and continued for up to 48 h. Ampicillin (100 μg/ml) and arabinose (0.2%, wt/vol) were used when needed. It should be noted that when biofilms are grown using a flow cell system with 2% LB supplemented with antibiotics, growth rate and biofilm formation are reduced relative to those of the biofilms formed in the absence of antibiotics. Following the biofilm growth period, the biofilms were either imaged directly or stained with Syto-9 (3.34 μM in phosphate-buffered saline [PBS]) prior to imaging (Life Technologies, Carlsbad, CA). Confocal images were obtained on a Zeiss LSM 5 Pascal laser scanning confocal microscope (Zeiss, Dublin, CA). Images were obtained with a 40× dry objective and were processed using Imaris software (Biplane, South Windsor, CT). Quantitative analyses were performed using the COMSTAT software package (32). Total biomass, average and maximum biofilm thicknesses, substrate coverage, and roughness coefficient were determined from *z*-stack images with the threshold set to 25. Five biofilm images were analyzed. Statistical significance was determined using Student's *t* test or one-way ANOVA with Dunnett's multiple-comparison test, when appropriate. Experiments with two biological replicates were carried out. Data presented are from one representative experiment.

Polymyxin B MIC assay. *V. cholerae* deletion and complemented strains were grown overnight aerobically at 30°C in LB medium with or without ampicillin (100 μg/ml), respectively. Cultures were diluted 1:200 in fresh LB medium (deletion strains) or LB medium supplemented with ampicillin (100 μg/ml) and arabinose (0.2%) (complementation strains), incubated aerobically at 30°C, and harvested when OD_{600} reached 0.5. To achieve confluent growth, the cultures were diluted 1:100 (deletion strains) or 1:10 (complementation strains) and 100 μl was plated onto appropriate agar medium. Etest gradient polymyxin B strips (bioMérieux, Durham, NC) were used to determine the polymyxin MIC of the strains after 24 h of incubation at 30°C. The polymyxin B killing assay was carried out according to a published protocol (2). Briefly, exponentially grown cells in LB or LB supplemented with 10 mM $CaCl_2$, pH 7.0 (18), were harvested, treated with 40 μg/ml polymyxin B for 1 h at 30°C, and plated. CFU were determined, and the percent survival was calculated as follow: % survival = $(CFU_{PMB\ treatment}/CFU_{no\ treatment}) \times 100$.

Infant mouse colonization assays. An *in vivo* competition assay for intestinal colonization was performed as described previously (33, 34). Each *V. cholerae* mutant strain (*lacZ*$^+$) and wild-type strain (*lacZ* minus) were grown to stationary phase at 30°C with aeration in LB broth. Individual mutant and wild-type strains were mixed at 1:1 ratios in 1× PBS. The inocula were plated on LB agar plates containing 5-bromo-4-chloro-3-indolyl-β-D-galactopyranoside (X-Gal) to differentiate wild-type and mutant colonies and to determine the input ratios. Approximately 10^6 to 10^7 CFU was intragastrically administered to groups of 5 to 7 anesthetized 5-day-old CD-1 mice (Charles River Laboratories, Hollister, CA). After 20 h of inoculation, the mice were sacrificed and the small intestine was removed, weighed, homogenized, and plated on appropriate selective and differential media to enumerate mutant and wild-type cells recovered, to determine the output ratios. *In vivo* competitive indices were calculated by dividing the small intestine output ratio by the inoculum input ratio of mutant to wild-type strains. Statistical analysis was performed using Student's *t* test. All animal procedures used were in strict accordance with the NIH *Guide for the Care and Use of Laboratory Animals* (35) and were approved by the UC Santa Cruz Institutional Animal Care and Use Committee (Yildf1206).

Luminescence assays. *V. cholerae* strains harboring the indicated plasmid were grown overnight in LB medium supplemented with 5 μg/ml chloramphenicol. Cells were then diluted 1:500 in fresh LB medium supplemented with 5 μg/ml chloramphenicol and harvested at exponential phase at an OD_{600} of 0.3 to 0.4. Luminescence was measured using a Victor3 multilabel counter (PerkinElmer, Waltham, MA), and *lux* expression is reported as counts min^{-1} ml^{-1}/OD_{600}. Assays were repeated with at least two biological replicates and four technical replicates.

RESULTS

CarR directly regulates the *almEFG* operon. Transcriptional profiling of *V. cholerae carR* and *carS* mutants revealed that the CarRS two-component system positively regulates expression of the *almEFG* genes (18). To confirm this finding, we quantified *almEFG* message levels by qRT-PCR. Expression of all three genes in the *almEFG* operon was significantly reduced (approximately 50-fold, $P \leq 0.01$) in the Δ*carR* strain compared to the wild-type strain (Fig. 1A). Complementation of the *carR* mutant with a wild-type copy of *carR*, provided on a pBAD plasmid, restored the expression of the *almEFG* operon to levels similar to those of the wild type. These findings support the hypothesis that CarR is an activator of the *almEFG* operon.

In order to determine if CarR directly regulates the expression of the *almEFG* operon, we analyzed the ability of a purified CarR to bind to the predicted regulatory region of the *almEFG* operon (Fig. 1B). We determined that CarR causes mobility shift of the predicted regulatory region of the *almEFG* operon (−250 to +160 bp with respect to the translational start site of *almE*), indicating that CarR binds to this region. We also observed direct binding of CarR to the *almEFG* promoter region spanning −100 to +54 bp with respect to the translational start site of *almE* (data not shown). Furthermore, we determined that CarR binding to the

TABLE 2 (Continued)

Mean (SD) and significance at[a]:									
48 h									
Biomass ($\mu m^3/\mu m^2$)	Significance	Avg thickness (μm)	Significance	Maximum thickness (μm)	Significance	Substrate coverage[b]	Significance	Roughness	Significance
20.51 (1.29)		20.39 (1.55)		29.70 (5.00)		1.00 (0.00)		0.09 (0.02)	
30.23 (3.14)	***	30.82 (3.76)	***	42.13 (5.16)	***	1.00 (0.00)	NS	0.08 (0.02)	NS
26.92 (2.82)	***	27.27 (2.53)	***	38.94 (5.36)	**	1.00 (0.00)	NS	0.09 (0.01)	NS
24.40 (1.37)	**	24.62 (1.70)	**	33.99 (3.08)	NS	1.00 (0.00)	NS	0.09 (0.01)	NS
20.55 (2.11)	NS	20.50 (1.74)	NS	30.47 (6.29)	NS	1.00 (0.00)	NS	0.10 (0.01)	NS
30.07 (1.82)	***	30.56 (2.05)	***	40.37 (2.68)	***	1.00 (0.00)	NS	0.08 (0.01)	NS

[a] Total biomass, average and maximum thicknesses, substrate coverage, and roughness coefficient were calculated using COMSTAT. Values presented are means of data from at least eight *z*-series image stacks. Significance was determined by an ANOVA (*P* values for 24 and 48 h are 0.0001 and 0.0002, respectively). Dunnett's multiple-comparison test identified samples that differ significantly from biofilms formed by the wild-type strain. NS, not significant; **, $P \leq 0.01$; ***, $P \leq 0.001$.
[b] A value of 0 indicates no coverage (equivalent to 0%), while a value of 1 indicates full coverage (equivalent to 100%).

regulatory region of the *almEFG* operon was specific. An excess (56×) of unlabeled specific probe was able to outcompete the formation of the CarR-$_{VIC}$*alm*$_{FAM}$ complex. In contrast, formation of the CarR-$_{VIC}$*alm*$_{FAM}$ complex was not affected by an excess (56×) probe consisting of the upstream region (−253 to −43 bp) of the *cyaA* gene, which is not regulated by the CarR response regulator (Fig. 1C). Taken together, these results show that CarR likely binds to the promoter region of the *almEFG* operon and regulates transcription of the *almEFG* operon directly.

The annotated intergenic region between the *almEFG* operon and VC1580 is 63 nucleotides long. To determine the minimal region required to promote expression of the *almEFG* operon, we generated transcriptional fusions to the promoterless *luxCDABE* operon carried in the pBBR*lux* plasmid. Transcriptional fusions starting at −250 (F1), −76 (F2), and −38 (F3) nucleotides upstream of the annotated *almE* translational start site were able to activate *lux* expression in wild-type *V. cholerae* (Fig. 1D and E). The highest level of expression is observed in strains harboring F1. The strains with the fusions F2 and F3 had a small but reproducible decrease in expression compared to the strains harboring F1. However, a fusion that begins at +1 (F4) lost the ability to promote expression of the *lux* reporter. Expression of F1 is abolished in a Δ*carR* strain. These results suggest that 38 nucleotides upstream of the annotated translational start site (F3) are sufficient to promote expression of the *almEFG* operon and that CarR is required for transcriptional activation. However, the promoter architecture of the *almEFG* operon has yet to be characterized in detail, and additional regulatory elements may be required for transcriptional activation.

CarR confers polymyxin B resistance through AlmEFG. It has been shown previously that *alm* mutants exhibit polymyxin B sensitivity compared to wild type (5). To investigate if a *carR* mutant also exhibits a similar polymyxin B sensitivity, the MIC of polymyxin B was determined in a *carR* mutant and the *alm* mutants (Fig. 2A) using Etest gradient polymyxin B strips. The *carR* mutant exhibited polymyxin B sensitivity, with a MIC of 1 μg/ml compared to the wild-type A1552, which exhibits a MIC of 48 μg/ml. The individual *alm* mutants, the triple *almEFG* mutant, and the quadruple *carR almEFG* mutants exhibited similar decreases in MIC (0.5 to 1 μg/ml). We also determined that a *carR* deletion in the *V. cholerae* C6706 genetic background resulted in a decrease in the MIC compared to that of its parental C6706 strain (Fig. 2A).

To further investigate if CarR-dependent polymyxin B resistance is mediated by AlmEFG, the polymyxin B MIC was determined in a *carR* mutant harboring an *almEFG* complementation plasmid (Fig. 2B). Expression of *almEFG* from the complementation plasmid rescued the polymyxin B sensitivity phenotype of the *carR* deletion mutant, indicating that CarR confers polymyxin B resistance via positive regulation of *almEFG*. As expected, the *carR* complementation plasmid was able to rescue the polymyxin B sensitivity of the *carR* mutant (0.75 μg/ml) to the wild-type level (96 μg/ml). Similarly, the polymyxin B-sensitive phenotype of the individual *alm* and triple *almEFG* deletion strains could be rescued to the wild-type level when the *alm* genes were expressed in *trans* from the complementation plasmids (Fig. 2B).

Calcium affects the susceptibility of *V. cholerae* to polymyxin B. Whole-genome expression profiling of *V. cholerae* cells grown in LB with Ca^{2+} (LBCa^{2+}) revealed that Ca^{2+} leads to a 2- to 3-fold decrease in transcription of *carR* and *alm* genes (18). Thus, we also compared the sensitivity of *V. cholerae* cells grown in LB supplemented with 10 mM Ca^{2+} to that of cells grown in LB, using polymyxin B killing assays (2) and Etest gradient polymyxin B strips. No significant difference in survival was observed when the wild-type A1552 strain grown in the presence and that grown in the absence of Ca^{2+} were exposed to polymyxin B (Fig. 2C). This finding suggests that the decreased *carR* and *alm* message abundance observed in wild-type bacteria grown in LBCa^{2+} does not lead to a reduction in polymyxin B resistance. In contrast, we observed an increase in polymyxin B MIC when wild-type A1552 cells were grown on LBCa^{2+} agar plates (Fig. 2D). Similarly, when Δ*carR* and Δ*almEFG* strains were treated with polymyxin B, both percent survival (Fig. 2C) and polymyxin B MIC (Fig. 2D) were significantly higher in the cells grown in the presence of Ca^{2+} than in cells grown in the absence of Ca^{2+}. These findings suggest that calcium modulates polymyxin B sensitivity via yet another unknown pathway that is independent of *carR* and *alm* operon products.

CarR impacts colonization in a strain-specific manner. Since CarR and AlmEFG confer resistance to polymyxin B, we wondered if they could also contribute to intestinal colonization. Therefore, we measured the ability of Δ*carR*, Δ*almE*, Δ*almF*,

Δ*almG*, and Δ*almEFG* mutants to colonize the infant mouse small intestine using a competition assay (Fig. 3). All the mutants generated in the *V. cholerae* A1552 genetic background colonized the infant mouse small intestine similarly to the wild-type strain. In contrast, the *carR* mutant in the C6706 genetic background showed a small but statistically significant difference in the levels of colonization from that of the wild-type strain. However, the Δ*almEFG* mutant in the C6706 genetic background did not exhibit defects in colonization. These results suggest that the contribution of CarR to colonization differs between the *V. cholerae* strains and that the Δ*carR* colonization defect in the C6706 genetic background is not due to decreased expression of *almEFG* operon genes.

AlmE impacts biofilm formation. Previous research in our laboratory has demonstrated that CarRS inhibits biofilm formation through repression of the *vps* operons and therefore VPS production (18). As discussed above, we demonstrated that CarR positively regulates expression of the *almEFG* operon. Thus, we wanted to test if *alm* genes impact biofilm formation. To this end, we analyzed biofilm-forming capabilities of the Δ*almE*, Δ*almF*, Δ*almG*, and Δ*almEFG* strains. Biofilms were grown using a flow cell system, imaged using CLSM, and analyzed using COMSTAT to evaluate biofilm structural properties. Quantitative analysis of biofilms revealed that 48 h postinoculation, biofilms formed by Δ*carR*, Δ*almE*, Δ*almF*, and Δ*almEFG* strains had significantly more biomass and greater average thickness than the wild-type biofilms (Fig. 4A; Table 2). The Δ*almG* mutant formed biofilms that were not significantly different from those of the wild type. Biofilms formed by a Δ*almEFG* mutant are similar to the biofilms formed by the Δ*almE* mutant, without an additive effect.

To further investigate the role of the *almEFG* operon in biofilm formation, we introduced a wild-type copy of the *alm* genes on the pBAD plasmid into their respective mutants and analyzed biofilm formation using a flow cell system (Fig. 4B). We observed that 30 h postinoculation, expression of *almE* from the pBAD promoter significantly reduced the biofilm biomass and average thickness compared to the *almE* mutant harboring an empty vector (Fig. 4B; Table 3). We also overexpressed individual *alm* genes from the pBAD promoter in wild-type A1552 and observed that overexpressing *almE* resulted in the most dramatic decreases in biofilm formation (data not shown). Collectively, these findings support the conclusion that AlmE is the primary regulator of biofilm formation in the *almEFG* operon.

To further test the effect of the *alm* genes in biofilm formation, we analyzed biofilm formation abilities of C6706 wild type and Δ*almE* and Δ*almEFG* mutants generated in the C6706 genetic background (Fig. 2C). COMSTAT analysis (Table 4) revealed that Δ*almE* and Δ*almEFG* mutants formed biofilms with increased biomass and thickness compared to biofilms formed by the C6706 wild-type strain. This finding shows that the effect of AlmE on biofilm formation is not strain specific.

AlmE negatively regulates *vps* gene expression. We previously reported that expression of *vpsL* is upregulated in the absence of *carR*. To evaluate if the observed biofilm phenotypes correlate with changes in expression of *vps* genes, we analyzed the expression of a *vpsLp-lux* transcriptional fusion in wild-type, Δ*carR*, Δ*almE*, Δ*almF*, Δ*almG*, and Δ*almEFG* strains (Fig. 5). As previously reported, expression of *vpsL* was upregulated in a Δ*carR* strain compared to wild type. Moreover, expression of *vpsL* is significantly upregulated in the Δ*almE* strain to levels higher

TABLE 3 COMSTAT quantitative analysis of biofilms formed after 30 h by wild-type A1552 harboring the empty vector and deletion strains harboring empty vector or complementation plasmids

Strain	Mean (SD) and significance[a]								
	Biomass ($\mu m^3/\mu m^2$)	Significance	Avg thickness (μm)	Significance	Maximum thickness (μm)	Significance	Substrate coverage	Significance	Roughness	Significance
Wild type with empty vector	9.56 (0.37)		8.83 (0.36)		23.32 (3.04)		0.995 (2.26×10^{-3})		0.375 (1.50×10^{-2})	
Δ*almE* mutant harboring										
Empty vector	7.80 (0.99)		7.27 (1.07)		19.71 (1.18)		0.879 (2.99×10^{-2})		0.435 (5.31×10^{-2})	
p*almE*	4.28 (1.21)	***	3.47 (1.22)	***	17.95 (6.24)	NS	0.943 (1.37×10^{-2})	**	0.589 (5.02×10^{-2})	**
Δ*almF* mutant harboring										
Empty vector	8.44 (0.66)		7.68 (0.64)		23.41 (0.79)		0.956 (2.23×10^{-2})		0.517 (5.41×10^{-2})	
p*almF*	6.83 (0.89)	NS	6.02 (0.91)	NS	24.20 (4.22)	NS	0.969 (8.39×10^{-3})	NS	0.551 (5.41×10^{-2})	NS
Δ*almG* mutant harboring										
Empty vector	8.37 (0.53)		7.57 (0.52)		22.88 (1.65)		0.978 (2.03×10^{-2})		0.494 (4.46×10^{-2})	
p*almG*	7.68 (0.43)	NS	6.90 (0.40)	NS	21.12 (3.11)	NS	0.953 (3.61×10^{-2})	NS	0.594 (8.86×10^{-2})	NS

[a] Total biomass, average and maximum thicknesses, substrate coverage, and roughness coefficient were calculated using COMSTAT. Values presented are means of data from at least five *z*-series image stacks. Significance was determined by Student's *t* test, comparing the mutant with the empty vector to the complemented strain. NS, not significant; **, $P \leq 0.01$; ***, $P \leq 0.001$.

TABLE 4 COMSTAT quantitative analysis of biofilms formed after 24 h by deletion strains in C6706 genetic background

Strain	Mean (SD) and significance[a]									
	Biomass ($\mu m^3/\mu m^2$)	Significance	Avg thickness (μm)	Significance	Maximum thickness (μm)	Significance	Substrate coverage	Significance	Roughness	Significance
C6706	16.27 (1.52)		16.68 (1.62)		35.75 (4.02)		1.00 (2.38×10^{-4})		0.36 (0.03)	
Δ*almE* mutant	20.85 (1.25)	***	22.97 (1.69)	***	40.26 (3.73)	*	1.00 (4.05×10^{-4})	NS	0.34 (0.02)	*
Δ*almEFG* mutant	20.13 (0.86)	***	21.77 (1.03)	***	38.50 (2.57)	NS	1.00 (1.70×10^{-4})	NS	0.34 (0.04)	*

[a] Total biomass, average and maximum thicknesses, substrate coverage, and roughness coefficient were calculated using COMSTAT. Values presented are means of data from at least eight *z*-series image stacks. Significance was determined by one-way ANOVA followed by Dunnett's multiple-comparison test, comparing the deletion mutants to the C6706 wild-type strain. NS, not significant; *, $P \leq 0.05$; ***, $P \leq 0.001$.

than those in the Δ*carR* strain. However, the expression of *vpsL* did not change in the Δ*almF* and Δ*almG* strains. The levels of expression of *vpsL* in the Δ*almEFG* strain are similar to the levels observed in the Δ*almE* strain. Upregulation of *vpsL* in the Δ*carR*, Δ*almE*, and Δ*almEFG* strains correlates with an increased ability to form biofilms.

DISCUSSION

V. cholerae is exposed to many environmental stresses in the human intestine, including changes in nutrient quality and quantity, oxygen levels, pH, temperature, bile, osmolarity, and host antimicrobial peptides. We report that CarR, the response regulator of the CarRS TCS, regulates resistance to the antimicrobial peptide polymyxin B in *V. cholerae*. Thus, *V. cholerae*, similarly to *S. enterica* serovar Typhimurium and *P. aeruginosa*, uses TCSs to regulate expression of genes involved in lipid A modification, and these pathways contribute to antimicrobial peptide resistance.

Our previous work showed that the expression of *carRS* and *almEFG* genes is downregulated in cells grown in LB medium supplemented with Ca^{2+}. Thus, we analyzed the effect of Ca^{2+} on polymyxin B resistance using polymyxin B killing assays and Etest gradient polymyxin B strips. We observed no significant difference in survival after exposure to polymyxin B when the wild-type A1552 strain was grown to exponential phase in LB alone or $LBCa^{2+}$. However, when we determined the MIC after 24 h of growth on LB and $LBCa^{2+}$ agar plates, MIC was increased in strains grown in the presence of Ca^{2+}. The observed differences in polymyxin B sensitivity in the two assays are likely due to the different growth states of the cells at the time of exposure to polymyxin B. It is important to note that a significant increase in MIC was also observed when the Δ*carR* and Δ*almEFG* strains were tested, indicating that Ca^{2+} levels modulate polymyxin B resistance independently of CarR and AlmEFG. At present, it is not known how divalent cations are sensed by *V. cholerae*. Activity of the histidine kinase PhoQ in *S. enterica* serovar Typhimurium is modulated by low extracellular concentrations of divalent cations Mg^{2+} and Ca^{2+}. Furthermore, it was shown that the extracellular DNA component of *S. enterica* serovar Typhimurium biofilm matrix activates PhoPQ/PmrAB systems and antimicrobial resistance by chelation of Mg^{2+} (36). Similarly, in *P. aeruginosa*, Mg^{2+} limitation promotes biofilm formation in a PhoPQ-dependent manner through modulation of the levels of small regulatory RNAs controlling biofilm formation (37). Two predicted *V. cholerae* PhoPQ homologs (VCA1104-05 and VC1638-39) might be involved in sensing divalent cations and associated antimicrobial resistance phenotypes.

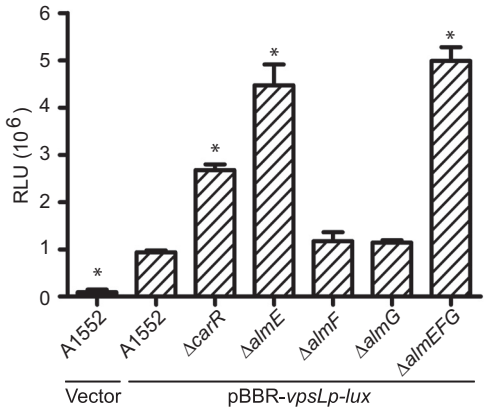

FIG 5 Analysis of *vpsL* expression in *alm* mutants. The expression of a *vpsLp-lux* transcriptional fusion was determined in wild-type, Δ*carR*, Δ*almE*, Δ*almF*, Δ*almG*, and Δ*almEFG* strains. The data represent the mean expression (relative luminescence units [RLU]) of four replicates from two independent experiments. The negative control, A1552 wild type harboring vector only, reflects the background luminescence obtained from the promoterless pBBR*lux* plasmid. Statistical significance was determined using a one-way ANOVA and Dunnett's multiple-comparison test. Asterisks indicate *P* values of <0.01. Error bars represent standard deviations.

We found that CarR contributes to intestinal colonization in a strain-specific manner. While the absence of CarR resulted in a small colonization defect in the *V. cholerae* O1 El Tor C6706 strain, it did not alter colonization in the *V. cholerae* O1 El Tor A1552 strain. At present, the genomic variation(s) responsible for differences in colonization is not known. Genome-wide transcriptional analyses of *V. cholerae* grown in an infant mouse model of infection have shown that expression of *carS* (VC1319) is induced during infection (38). It is possible that CarRS, as an infection-induced TCS, affects adaptation to the host environment and to host antimicrobial peptides. Neonatal mice could produce the cathelin-related antimicrobial peptide (CRAMP) (39), and CarR could be involved in resistance to CRAMP. We determined that AlmEFG did not contribute to intestinal colonization. However, contribution of CarR or AlmEFG to the general response to antimicrobial peptides has yet to be evaluated. Alternatively, another gene(s) whose expression is controlled by CarR could contribute to intestinal colonization.

Modifications to LPS, the major component of the outer mem-

brane of Gram-negative bacteria, have been shown to affect biofilm formation in *P. aeruginosa* and *E. coli* (40, 41). The impact of modifications to LPS on *V. cholerae* biofilm formation and biofilm physiology has not been previously studied. We found that mainly AlmE and, to a smaller extent, AlmF could downregulate biofilm formation. This would suggest that the absence of *almE*, but not necessarily the absence of glycine modification at lipid A, promotes an increase in biofilm formation and an upregulation of *vpsL*. It was proposed that AlmE functions as an amino acid ligase and AlmF functions as a glycine carrier protein. AlmE catalyzes glycine ligation as a thioester to the cognate carrier protein AlmF. AlmG then catalyzes the transfer of glycine to the unmodified hexa-acylated *V. cholerae* lipid A (5). AlmE was initially annotated as an enterobactin synthetase component F-related protein and harbors an amino acid adenylation domain found in nonribosomal peptide synthetases (NRPS) involved in the biosynthesis of siderophores. AlmF shows structural similarity to acyl-acyl carrier protein (ACP) (5). NRPS act in conjunction with peptidyl carrier proteins (PCPs) or aryl carrier proteins (ArCPs). It is possible that in addition to their role in the synthesis of glycine-modified lipid A species, AlmE and AlmF could participate in the biosynthesis of a novel compound that affects biofilm formation. The biochemical characterization of AlmEFG and the substrate specificity for these proteins have to be assessed to gain a complete understanding of the role of AlmEFG proteins in *V. cholerae* biofilm formation. Further work is also needed to understand which environmental signals are sensed by the CarRS TCS to control *almEFG* expression and in turn antimicrobial resistance and biofilm formation.

ACKNOWLEDGMENTS

We thank Benjamin Abrams from the UCSC Life Sciences Microscopy Center for his technical support and Jennifer Teschler for her comments on the manuscript.

This work was supported by the NIH grant R01AI055987.

REFERENCES

1. **Zasloff M.** 2002. Antimicrobial peptides of multicellular organisms. Nature **415:**389–395. http://dx.doi.org/10.1038/415389a.
2. **Matson JS, Yoo HJ, Hakansson K, Dirita VJ.** 2010. Polymyxin B resistance in El Tor *Vibrio cholerae* requires lipid acylation catalyzed by MsbB. J Bacteriol **192:**2044–2052. http://dx.doi.org/10.1128/JB.00023-10.
3. **Mathur J, Waldor MK.** 2004. The *Vibrio cholerae* ToxR-regulated porin OmpU confers resistance to antimicrobial peptides. Infect Immun **72:**3577–3583. http://dx.doi.org/10.1128/IAI.72.6.3577-3583.2004.
4. **Mathur J, Davis BM, Waldor MK.** 2007. Antimicrobial peptides activate the *Vibrio cholerae* sigmaE regulon through an OmpU-dependent signalling pathway. Mol Microbiol **63:**848–858. http://dx.doi.org/10.1111/j.1365-2958.2006.05544.x.
5. **Hankins JV, Madsen JA, Giles DK, Brodbelt JS, Trent MS.** 2012. Amino acid addition to *Vibrio cholerae* LPS establishes a link between surface remodeling in gram-positive and gram-negative bacteria. Proc Natl Acad Sci U S A **109:**8722–8727. http://dx.doi.org/10.1073/pnas.1201313109.
6. **Hankins JV, Madsen JA, Giles DK, Childers BM, Klose KE, Brodbelt JS, Trent MS.** 2011. Elucidation of a novel *Vibrio cholerae* lipid A secondary hydroxy-acyltransferase and its role in innate immune recognition. Mol Microbiol **81:**1313–1329. http://dx.doi.org/10.1111/j.1365-2958.2011.07765.x.
7. **Bina XR, Provenzano D, Nguyen N, Bina JE.** 2008. *Vibrio cholerae* RND family efflux systems are required for antimicrobial resistance, optimal virulence factor production, and colonization of the infant mouse small intestine. Infect Immun **76:**3595–3605. http://dx.doi.org/10.1128/IAI.01620-07.
8. **Gao R, Stock AM.** 2009. Biological insights from structures of two-component proteins. Annu Rev Microbiol **63:**133–154. http://dx.doi.org/10.1146/annurev.micro.091208.073214.
9. **Stock AM, Robinson VL, Goudreau PN.** 2000. Two-component signal transduction. Annu Rev Biochem **69:**183–215. http://dx.doi.org/10.1146/annurev.biochem.69.1.183.
10. **Laub MT, Goulian M.** 2007. Specificity in two-component signal transduction pathways. Annu Rev Genet **41:**121–145. http://dx.doi.org/10.1146/annurev.genet.41.042007.170548.
11. **Trent MS, Pabich W, Raetz CR, Miller SI.** 2001. A PhoP/PhoQ-induced lipase (PagL) that catalyzes 3-O-deacylation of lipid A precursors in membranes of *Salmonella typhimurium*. J Biol Chem **276:**9083–9092. http://dx.doi.org/10.1074/jbc.M010730200.
12. **Guo L, Lim KB, Poduje CM, Daniel M, Gunn JS, Hackett M, Miller SI.** 1998. Lipid A acylation and bacterial resistance against vertebrate antimicrobial peptides. Cell **95:**189–198. http://dx.doi.org/10.1016/S0092-8674(00)81750-X.
13. **Bader MW, Navarre WW, Shiau W, Nikaido H, Frye JG, McClelland M, Fang FC, Miller SI.** 2003. Regulation of *Salmonella typhimurium* virulence gene expression by cationic antimicrobial peptides. Mol Microbiol **50:**219–230. http://dx.doi.org/10.1046/j.1365-2958.2003.03675.x.
14. **Gunn JS, Miller SI.** 1996. PhoP-PhoQ activates transcription of *pmrAB*, encoding a two-component regulatory system involved in *Salmonella typhimurium* antimicrobial peptide resistance. J Bacteriol **178:**6857–6864.
15. **Gunn JS, Lim KB, Krueger J, Kim K, Guo L, Hackett M, Miller SI.** 1998. PmrA-PmrB-regulated genes necessary for 4-aminoarabinose lipid A modification and polymyxin resistance. Mol Microbiol **27:**1171–1182. http://dx.doi.org/10.1046/j.1365-2958.1998.00757.x.
16. **McPhee JB, Lewenza S, Hancock RE.** 2003. Cationic antimicrobial peptides activate a two-component regulatory system, PmrA-PmrB, that regulates resistance to polymyxin B and cationic antimicrobial peptides in *Pseudomonas aeruginosa*. Mol Microbiol **50:**205–217. http://dx.doi.org/10.1046/j.1365-2958.2003.03673.x.
17. **Fernandez L, Gooderham WJ, Bains M, McPhee JB, Wiegand I, Hancock RE.** 2010. Adaptive resistance to the "last hope" antibiotics polymyxin B and colistin in *Pseudomonas aeruginosa* is mediated by the novel two-component regulatory system ParR-ParS. Antimicrob Agents Chemother **54:**3372–3382. http://dx.doi.org/10.1128/AAC.00242-10.
18. **Bilecen K, Yildiz FH.** 2009. Identification of a calcium-controlled negative regulatory system affecting *Vibrio cholerae* biofilm formation. Environ Microbiol **11:**2015–2029. http://dx.doi.org/10.1111/j.1462-2920.2009.01923.x.
19. **Fong JC, Syed KA, Klose KE, Yildiz FH.** 2010. Role of *Vibrio* polysaccharide (*vps*) genes in VPS production, biofilm formation and *Vibrio cholerae* pathogenesis. Microbiology **156:**2757–2769. http://dx.doi.org/10.1099/mic.0.040196-0.
20. **Fong JC, Karplus K, Schoolnik GK, Yildiz FH.** 2006. Identification and characterization of RbmA, a novel protein required for the development of rugose colony morphology and biofilm structure in *Vibrio cholerae*. J Bacteriol **188:**1049–1059. http://dx.doi.org/10.1128/JB.188.3.1049-1059.2006.
21. **Fong JC, Yildiz FH.** 2007. The *rbmBCDEF* gene cluster modulates development of rugose colony morphology and biofilm formation in *Vibrio cholerae*. J Bacteriol **189:**2319–2330. http://dx.doi.org/10.1128/JB.01569-06.
22. **Berk V, Fong JC, Dempsey GT, Develioglu ON, Zhuang X, Liphardt J, Yildiz FH, Chu S.** 2012. Molecular architecture and assembly principles of *Vibrio cholerae* biofilms. Science **337:**236–239. http://dx.doi.org/10.1126/science.1222981.
23. **Yildiz FH, Visick KL.** 2009. *Vibrio* biofilms: so much the same yet so different. Trends Microbiol **17:**109–118. http://dx.doi.org/10.1016/j.tim.2008.12.004.
24. **Beyhan S, Bilecen K, Salama SR, Casper-Lindley C, Yildiz FH.** 2007. Regulation of rugosity and biofilm formation in *Vibrio cholerae*: comparison of VpsT and VpsR regulons and epistasis analysis of *vpsT*, *vpsR*, and *hapR*. J Bacteriol **189:**388–402. http://dx.doi.org/10.1128/JB.00981-06.
25. **Yildiz FH, Dolganov NA, Schoolnik GK.** 2001. VpsR, a member of the response regulators of the two-component regulatory systems, is required for expression of *vps* biosynthesis genes and EPS(ETr)-associated phenotypes in *Vibrio cholerae* O1 El Tor. J Bacteriol **183:**1716–1726. http://dx.doi.org/10.1128/JB.183.5.1716-1726.2001.
26. **Casper-Lindley C, Yildiz FH.** 2004. VpsT is a transcriptional regulator required for expression of *vps* biosynthesis genes and the development of rugose colonial morphology in *Vibrio cholerae* O1 El Tor. J Bacteriol **186:**1574–1578. http://dx.doi.org/10.1128/JB.186.5.1574-1578.2004.
27. **Hammer BK, Bassler BL.** 2003. Quorum sensing controls biofilm forma-

tion in *Vibrio cholerae*. Mol Microbiol **50:**101–104. http://dx.doi.org/10.1046/j.1365-2958.2003.03688.x.
28. **Yildiz FH, Liu XS, Heydorn A, Schoolnik GK.** 2004. Molecular analysis of rugosity in a *Vibrio cholerae* O1 El Tor phase variant. Mol Microbiol **53:**497–515. http://dx.doi.org/10.1111/j.1365-2958.2004.04154.x.
29. **Zhu J, Mekalanos JJ.** 2003. Quorum sensing-dependent biofilms enhance colonization in *Vibrio cholerae*. Dev Cell **5:**647–656. http://dx.doi.org/10.1016/S1534-5807(03)00295-8.
30. **Fong JC, Yildiz FH.** 2008. Interplay between cyclic AMP-cyclic AMP receptor protein and cyclic di-GMP signaling in *Vibrio cholerae* biofilm formation. J Bacteriol **190:**6646–6659. http://dx.doi.org/10.1128/JB.00466-08.
31. **Pfaffl MW.** 2001. A new mathematical model for relative quantification in real-time RT-PCR. Nucleic Acids Res **29:**e45. http://dx.doi.org/10.1093/nar/29.9.e45.
32. **Heydorn A, Nielsen AT, Hentzer M, Sternberg C, Givskov M, Ersboll BK, Molin S.** 2000. Quantification of biofilm structures by the novel computer program COMSTAT. Microbiology **146:**2395–2407.
33. **Freter R, O'Brien PC, Macsai MS.** 1981. Role of chemotaxis in the association of motile bacteria with intestinal mucosa: *in vivo* studies. Infect Immun **34:**234–240.
34. **Lee SH, Angelichio MJ, Mekalanos JJ, Camilli A.** 1998. Nucleotide sequence and spatiotemporal expression of the *Vibrio cholerae vieSAB* genes during infection. J Bacteriol **180:**2298–2305.
35. **National Research Council.** 2011. Guide for the care and use of laboratory animals, 8th ed. National Academies Press, Washington, DC.
36. **Johnson L, Horsman SR, Charron-Mazenod L, Turnbull AL, Mulcahy H, Surette MG, Lewenza S.** 2013. Extracellular DNA-induced antimicrobial peptide resistance in *Salmonella enterica* serovar Typhimurium. BMC Microbiol **13:**115. http://dx.doi.org/10.1186/1471-2180-13-115.
37. **Mulcahy H, Lewenza S.** 2011. Magnesium limitation is an environmental trigger of the *Pseudomonas aeruginosa* biofilm lifestyle. PLoS One **6:**e23307. http://dx.doi.org/10.1371/journal.pone.0023307.
38. **Mandlik A, Livny J, Robins WP, Ritchie JM, Mekalanos JJ, Waldor MK.** 2011. RNA-Seq-based monitoring of infection-linked changes in *Vibrio cholerae* gene expression. Cell Host Microbe **10:**165–174. http://dx.doi.org/10.1016/j.chom.2011.07.007.
39. **Menard S, Forster V, Lotz M, Gutle D, Duerr CU, Gallo RL, Henriques-Normark B, Putsep K, Andersson M, Glocker EO, Hornef MW.** 2008. Developmental switch of intestinal antimicrobial peptide expression. J Exp Med **205:**183–193. http://dx.doi.org/10.1084/jem.20071022.
40. **Lau PC, Lindhout T, Beveridge TJ, Dutcher JR, Lam JS.** 2009. Differential lipopolysaccharide core capping leads to quantitative and correlated modifications of mechanical and structural properties in *Pseudomonas aeruginosa* biofilms. J Bacteriol **191:**6618–6631. http://dx.doi.org/10.1128/JB.00698-09.
41. **Nakao R, Ramstedt M, Wai SN, Uhlin BE.** 2012. Enhanced biofilm formation by *Escherichia coli* LPS mutants defective in Hep biosynthesis. PLoS One **7:**e51241. http://dx.doi.org/10.1371/journal.pone.0051241.
42. **Herrero M, de Lorenzo V, Timmis KN.** 1990. Transposon vectors containing non-antibiotic resistance selection markers for cloning and stable chromosomal insertion of foreign genes in gram-negative bacteria. J Bacteriol **172:**6557–6567.
43. **de Lorenzo V, Timmis KN.** 1994. Analysis and construction of stable phenotypes in gram-negative bacteria with Tn5- and Tn10-derived minitransposons. Methods Enzymol **235:**386–405. http://dx.doi.org/10.1016/0076-6879(94)35157-0.
44. **Taylor RK, Manoil C, Mekalanos JJ.** 1989. Broad-host-range vectors for delivery of Tn*phoA*: use in genetic analysis of secreted virulence determinants of *Vibrio cholerae*. J Bacteriol **171:**1870–1878.
45. **Yildiz FH, Schoolnik GK.** 1999. *Vibrio cholerae* O1 El Tor: identification of a gene cluster required for the rugose colony type, exopolysaccharide production, chlorine resistance, and biofilm formation. Proc Natl Acad Sci U S A **96:**4028–4033. http://dx.doi.org/10.1073/pnas.96.7.4028.
46. **Beyhan S, Tischler AD, Camilli A, Yildiz FH.** 2006. Differences in gene expression between the classical and El Tor biotypes of *Vibrio cholerae* O1. Infect Immun **74:**3633–3642. http://dx.doi.org/10.1128/IAI.01750-05.
47. **Marsh JW, Sun D, Taylor RK.** 1996. Physical linkage of the *Vibrio cholerae* mannose-sensitive hemagglutinin secretory and structural subunit gene loci: identification of the *mshG* coding sequence. Infect Immun **64:**460–465.
48. **Hammer BK, Bassler BL.** 2007. Regulatory small RNAs circumvent the conventional quorum sensing pathway in pandemic *Vibrio cholerae*. Proc Natl Acad Sci U S A **104:**11145–11149. http://dx.doi.org/10.1073/pnas.0703860104.
49. **Bao Y, Lies DP, Fu H, Roberts GP.** 1991. An improved Tn7-based system for the single-copy insertion of cloned genes into chromosomes of gram-negative bacteria. Gene **109:**167–168. http://dx.doi.org/10.1016/0378-1119(91)90604-A.